Journal of Solid State Chemistry 181 (2008) 2852–2858

Contents lists available at ScienceDirect

Journal of Solid State Chemistry

journal homepage: www.elsevier.com/locate/jssc

# Synthesis of molecular imprinted polymer modified $TiO_2$ nanotube array electrode and their photoelectrocatalytic activity

Na Lu, Shuo Chen, Hongtao Wang, Xie Quan *, Huimin Zhao

*Key Laboratory of Industrial Ecology and Environmental Engineering (Ministry of Education, China), School of Environmental and Biological Science and Technology, Dalian University of Technology, Dalian 116024, China*

ARTICLE INFO

*Article history:*
Received 27 February 2008
Received in revised form
2 July 2008
Accepted 7 July 2008
Available online 15 July 2008

*Keywords:*
Molecular imprinted polymers
$TiO_2$ nanotube array electrode
Tetracycline hydrochloride
Photoelectrocatalysis

ABSTRACT

A tetracycline hydrochloride (TC) molecularly imprinted polymer (MIP) modified $TiO_2$ nanotube array electrode was prepared via surface molecular imprinting. Its surface was structured with surface voids and the nanotubes were open at top end with an average diameter of approximately 50 nm. The MIP-modified $TiO_2$ nanotube array with anatase phase was identified by XRD and a distinguishable red shift in the absorption spectrum was observed. The MIP-modified electrode also exhibited a high adsorption capacity for TC due to its high surface area providing imprinted sites. Photocurrent was generated on the MIP-modified photoanode using the simulated solar spectrum and increased with the increase of positive bias potential. Under simulated solar light irradiation, the MIP-modified $TiO_2$ nanotube array electrode exhibited enhanced photoelectrocatalytic (PEC) activity with the apparent first-order rate constant being 1.2-fold of that with $TiO_2$ nanotube array electrode. The effect of the thickness of the MIP layer on the PEC activity was also evaluated.



## 1. Introduction

Photoelectrocatalytic (PEC) oxidation has been reported as an efficient method in improving the photocatalytic (PC) efficiency of the photoelectrode by applying a low electrical bias potential between the anode and the cathode, which can decrease the recombination rate of photogenerated electrons and holes [1–3]. A stable and active photoelectrode is crucial in obtaining good PEC performance. $TiO_2$ has been proved to be a promising photocatalyst because of its high PC activity. The $TiO_2$ photoelectrode, which is prepared by immobilizing $TiO_2$ on a solid carrier, is widely used in PEC oxidation. Some supported carriers, in particular copper, aluminum and stainless steels, were more easily oxidized under a positive bias, even without UV illumination [4,5]. By comparison, titanium has become a kind of favorable carrier for coating $TiO_2$ photocatalyst to be used as photoelectrode, for the possible reason that titanium oxidizes only at applied potentials higher than 3 V [6].

In recent years, highly ordered $TiO_2$ nanotube array produced by potentiostatic anodization has become a kind of interesting inorganic material due to its large internal surface area. Its well-formed nanotube-array architecture offers the ability to influence the absorption and propagation of light through the architecture, and the closely packed vertically aligned crystalline tubes also offer the excellent electron percolation pathways for vectorial charge transfer between interfaces [7–9]. Because the $TiO_2$ nanotube array grows directly on the titanium substrate by electrochemical anodic oxidation method, it possesses a very strong mechanical strength [10]. So the anodic $TiO_2$ nanotube is a stable photocatalyst in the solution and has displayed excellent PC and PEC performances under UV light irradiation [3,10].

Adsorption of the organic pollutants over $TiO_2$ photocatalyst is usually considered to be an important parameter in determining degradation rates of PC oxidation [11] and surface modification may be an alternative strategy to increase the adsorption ability of $TiO_2$. Molecular imprinting is a promising technique for creating specific molecular recognition sites in solid materials by using template molecules [12]. Since Mosbach and co-workers reported the theophylline and diazepam molecularly imprinted polymer (MIP) for mimicking the antibody combining sites [13], interest in the molecular imprinting technique has surged because of its unique properties of predetermination, selectivity and specific affinity for the template [14–18]. In general, the MIP synthesis undergoes three steps, viz. mixing the functional monomers and the template, polymerization of a monomer with a cross-linker around a template molecule through UV light irradiation or calefaction way, and lastly, removing the template by washing. In this way, the sites capable of selectively rebinding the target analyte are left in the polymer [17,19]. Nowadays, the combination of surface molecular assembly with nanostructures in the

* Corresponding author. Fax: +86 411 84706263.
*E-mail address:* quanxie@dlut.edu.cn (X. Quan).

0022-4596/$ - see front matter © 2008 Elsevier Inc. All rights reserved.
doi:10.1016/j.jssc.2008.07.004

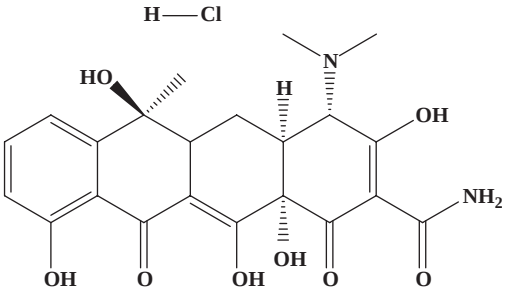


**Fig. 1.** Chemical structure of tetracycline hydrochloride.

imprinting technology and imprinting template molecules at single-hole hollow microspheres have been developed to take advantage of large surface areas for increasing the imprinting sites effectively [12,20,21], and the molecularly imprinted materials have showed potential applications not only in sensors, separation and bioassay [16,17,22–25], but also in photocatalysis. Recently, Zhu and co-workers prepared MIP-modified $TiO_2$ photocatalyst and found that the PC activity of $TiO_2$ was improved [26,27]. However, they used P25 as the carrier, which would suffer from the difficulty of separating suspended $TiO_2$ particles from aqueous solution.

The $TiO_2$ nanotubes have improved properties compared to any other forms of titania [28], among which the anodic $TiO_2$ nanotube arrays have the most remarkable properties. The strategy of increasing the adsorption capability of $TiO_2$ nanotube array electrode by modifying it via a thin layer of MIP becomes accessible to construct a novel MIP-$TiO_2$ hybrid electrode, which keeps both a specific adsorption capacity and high PEC activity. To our knowledge, application of MIP-modified $TiO_2$ nanotube array electrode in PEC degradation has not been reported. Antibiotics have been exposed to the environment with increasing attention. The excessive accumulation of tetracycline hydrochloride (TC; see Fig. 1), a type of broad-spectrum antibiotic, can produce a series of pathological changes and disrupt ecosystem equilibrium [29,30]. In the present study, MIP-modified $TiO_2$ nanotube array electrode was prepared, using TC as the template and the test substance as well. The MIP-modified $TiO_2$ nanotube array may find its important roles in enhancing the PEC activity of $TiO_2$ for the degradation of pollutants.

## 2. Experimental

### 2.1. Chemicals and materials

The titanium sheets were purchased from Tianjin Gerui Co. Ltd., China. Tetracycline hydrochloride (TC) and ethylene glycol dimethacrylate (EGDMA) were obtained from Alfa Aesar A Johnson Matthey, United States. Methacrylic acid (MAA) was from Tianjin Bodi Chemical Ltd., China, and 2,2′-azobisisobutyronitrile (AIBN) was from Tianjin Fuchen Chemical Reagent Co., China. All the other chemicals were of analytical grade and used as received. Deionized water was used for preparation of all aqueous solutions.

### 2.2. Preparation of $TiO_2$ nanotube arrays

The anodization of pretreated titanium sheet was performed in a two-electrode electrochemical cell. More details of anodic oxidation had been described previously [31]. To induce crystallinity, the initially amorphous as-anodized sample was annealed at 500 °C for 1 h with heating and cooling rates of 2 °C $min^{-1}$.

### 2.3. Preparation of MIP-modified $TiO_2$ nanotube arrays

The imprinted polymer was prepared by radical polymerization method. The template molecule, functional monomer, cross-linker and initiator were dissolved in 1 mL of methanol in a columniform quartz tube to make a mixture solution containing 0.013 M TC, 0.36 M MAA, 1.79 M EGDMA and 0.054 M AIBN. The solution was mixed uniformly by sonication for 5 min, and then was slowly dropped on two sides of $TiO_2$ nanotube array electrode to get a uniform coating. Afterwards, the electrode was fixed in the columniform quartz tube. The tube was then sealed and purged with nitrogen for a further 20 min. Polymerization was carried out under UV light irradiation for 4 h. The template was removed by successive washing in deionized water until no TC was detected in the eluates. At the same time, the nonimprinted (NIP)-modified $TiO_2$ nanotube array electrode was prepared as a reference using the same reaction mixture without the addition of the template and being treated in the same procedure.

### 2.4. Characterization of MIP-modified $TiO_2$ nanotube arrays

Atomic force microscopy (AFM; CSPM, Being Nano-Instruments Ltd.) was used to scan the MIP-layer surface structure of the MIP-modified $TiO_2$ nanotube arrays over an area of 5 μm × 5 μm. Morphological characterization of the samples was carried out using environmental scanning electron microscope (ESEM; Quanta 200 FEG). X-ray diffraction (XRD) analysis using a diffractometer with Cu $K\alpha$ radiation (Shimadzu LabX XRD-6000) was used to determine the crystalline structure of the samples. The UV–vis diffuse reflectance spectra (DRS) were recorded on a Jasco UV-550 spectrophotometer with an integrating sphere; $BaSO_4$ was used as a reference sample.

### 2.5. Photoelectrochemical measurements

The photocurrent density was measured using a CHI electrochemical analyzer (CH Instruments 650B, Shanghai Chenhua Instrument Co. Ltd., China) in a standard three-electrode configuration with the MIP-modified sample as photoanode, a platinum foil as counter electrode and a saturated calomel electrode (SCE) as reference electrode. A high-pressure xenon short arc lamp (CHF-XM35-150 W, Beijing Changtuo Co. Ltd., China), as a spectra physics solar simulator, was applied as the radiation source.

### 2.6. Photoelectrocatalytic experiment

The PEC oxidation of TC was carried out in a single photoelectrochemical compartment. The MIP-modified $TiO_2$ nanotube array as photoanode, a platinum foil as counter electrode and an SCE as reference electrode were connected to the CHI 650B electrochemical analyzer. Bias potentials applied on the photoanode were 0.4 V (vs. SCE) in the experiments. The spectra physics solar simulator (CHF-XM35-500 W, Beijing Changtuo Co. Ltd., China) with the illumination intensity of 100 mW $cm^{-2}$, which was measured by a radiometer (model FZ-A, Photoelectric Instrument Factory, Beijing Normal University, China) at the position of photoanode, was placed in parallel with the photoreactor. All the experiments went on with continuous magnetic stirring. The initial concentration of TC aqueous solution (40 mL) was 5 mg $L^{-1}$ and 0.01 M sodium sulfate was added as the electrolyte. During the reaction, the TC solution was sampled periodically and the absorbance was measured at 277 nm using a Jasco V-550 spectrophotometer. A total organic carbon (TOC) analyzer (TOC-$V_{CPH}$, Shimadzu, Japan) was employed for determining the mineralization of TC solutions.

## 3. Results and discussion

### 3.1. Surface of the MIP modified on the $TiO_2$ nanotube array electrode

Fig. 2 shows AFM images of the surface of the MIP modified on the $TiO_2$ nanotube array electrodes. An MIP layer covered on the surface of the electrode can be seen obviously in Fig. 2(a). The rugged surface of the cross-linked MIP before being washed by water presented a pattern of crests and valleys. As shown in Fig. 2(b), more surface voids were observed after the electrode being washed with deionized water, which could be ascribed to the removal of the template as well as the volatilization of the solvent [19]. The role of the solvent in the molecular imprinted technology is to provide porous structure for the MIP. During the process of polymerization, the solvent molecules can enter the inside of the MIP and are removed in the post treatment, leaving pores in the MIP. They can not only hasten both the bonding rate of template molecule with the monomer and the removal rate of the template molecule, but also promote the electron transfer between the electrolyte solution and the surface of the $TiO_2$ nanotube array electrode [19].

### 3.2. Morphology of the MIP-modified $TiO_2$ nanotube arrays

Fig. 3 shows the top-view ESEM images of neat and MIP-modified $TiO_2$ nanotube arrays. The electrodes modified with different thicknesses of MIP layer, namely thin and thick MIP layers, were obtained using approximately 200 and 800 μL of the same mixture solutions of polymerization precursors, respectively, which were continuously dropped on each side of the $TiO_2$ nanotube array electrodes, and being treated in the same procedure. From Fig. 3(b), most nanotubes of MIP-modified electrode were still open at the top end, the same as the $TiO_2$ nanotubes (Fig. 3(a)). In the process of MIP modification, the mixture solution could diffuse down the length of the hollow core of the nanotubes; thus, the inside surface of the nanotubes was modified with the thin MIP layer, making the average diameter reduced from approximately 80 to 50 nm. While further increasing the thickness of the MIP layers, the $TiO_2$ nanotube pores were blocked deeply (Fig. 3(c)) and the surface area was decreased, leading a reduction of the PEC activity of MIP-modified electrode. Accordingly, the $TiO_2$ nanotube array electrode modified with thin MIP layer was chosen for the following investigations in the present study.

### 3.3. XRD analysis

Fig. 4 corresponds to XRD patterns obtained from $TiO_2$ nanotube arrays and MIP-modified $TiO_2$ nanotube arrays. The XRD patterns of as-anodized $TiO_2$ nanotube arrays were found to be amorphous in nature and were annealed to convert them to crystalline phases as seen in Fig. 4(a). The MIP-modified $TiO_2$ nanotube arrays had crystallized structure (Fig. 4(b)) with clear

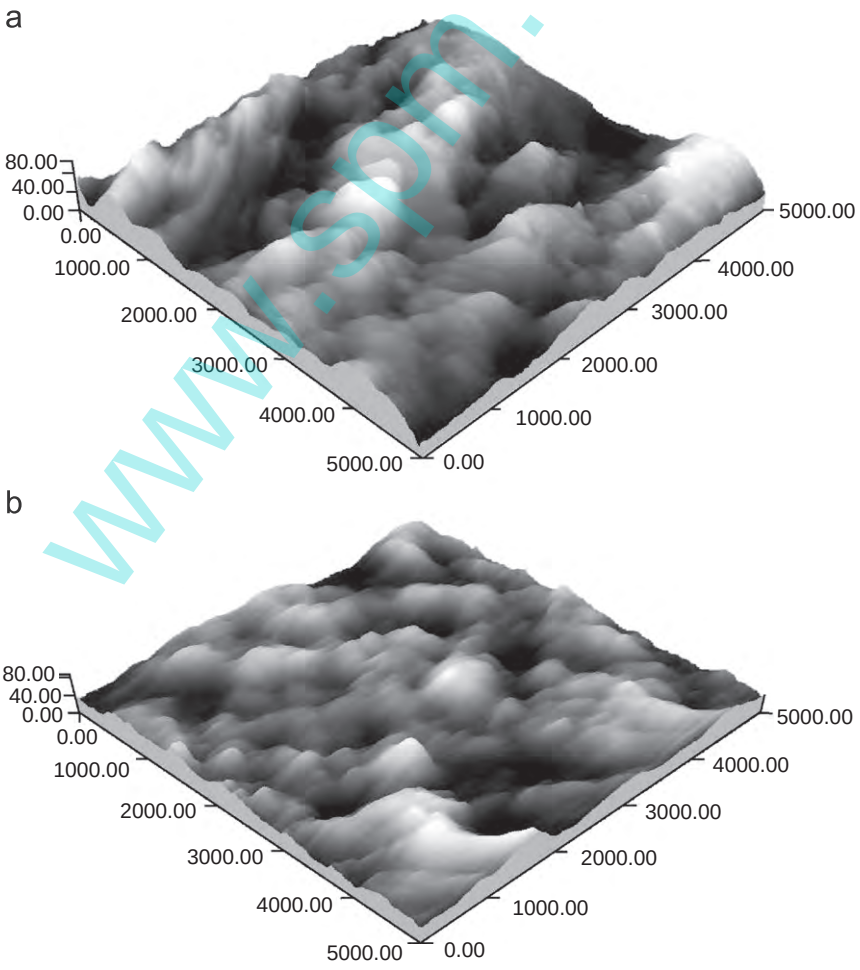


**Fig. 2.** AFM images of the surfaces of the MIP layer modified on $TiO_2$ nanotube array electrode: (a) before being washed by deionized water and (b) after being washed by deionized water.

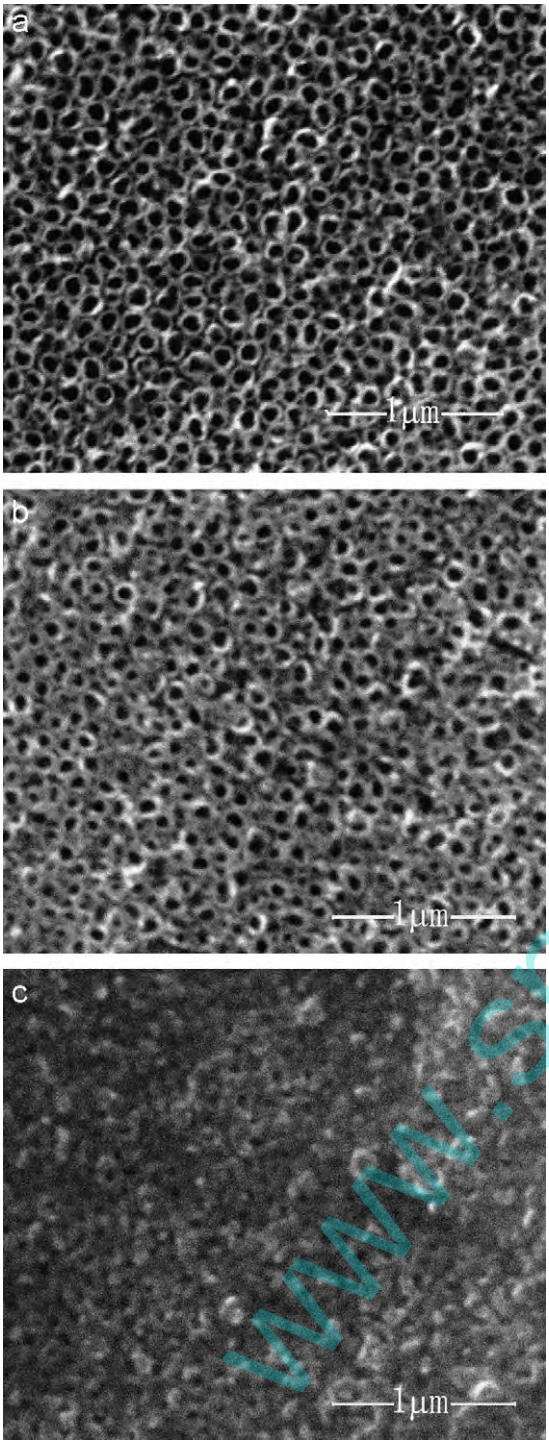


**Fig. 3.** Top-view ESEM images of: (a) $TiO_2$ nanotube arrays and $TiO_2$ nanotube arrays modified with (b) thin MIP layer and (c) thick MIP layer.

diffraction of anatase ($2\theta = 25.2^\circ$), which were almost the same as $TiO_2$ nanotube arrays. The results of XRD patterns indicated that the process of modifying MIP layer on the $TiO_2$ nanotube arrays did not affect its crystallization.

### 3.4. DRS analysis

The anodic $TiO_2$ nanotube array electrode has been proved to have higher PEC activity than that of $TiO_2$ layer electrode under

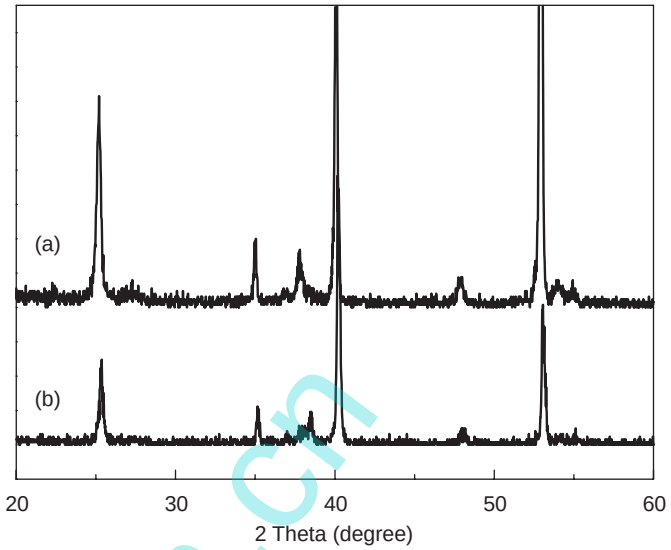


**Fig. 4.** XRD patterns of: (a) $TiO_2$ nanotube arrays and (b) MIP-modified $TiO_2$ nanotube arrays.

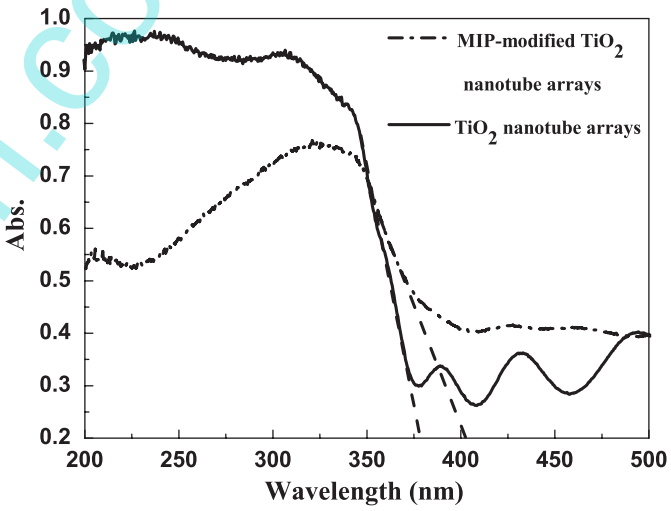


**Fig. 5.** DRS spectra of MIP-modified $TiO_2$ nanotube arrays and $TiO_2$ nanotube arrays.

UV light irradiation [3]; however, its band gap energy is so wide that it offers relatively inefficient utilization of solar energy. In the present study, we found that the MIP-modified $TiO_2$ nanotube arrays showed enhanced visible-light response than $TiO_2$ nanotube arrays. As shown in Fig. 5, a distinguishable red shift in the absorption spectrum of MIP-modified $TiO_2$ nanotube arrays was observed. Compared to $TiO_2$ nanotube arrays, the absorption edge moved from 378 to 403 nm. Therefore, we can assume an improved PEC activity of MIP-modified $TiO_2$ nanotube array electrode under solar light irradiation. According to the UV–vis DRS spectra, it is suggested that the process of modifying $TiO_2$ nanotube arrays with a thin MIP layer provided a possibility to combine photocatalysis with solar energy effectively.

### 3.5. The adsorption property of MIP-modified $TiO_2$ nanotube arrays

The adsorption of TC on MIP-modified $TiO_2$ nanotube arrays was performed by placing the sample in the solutions (40 mL)

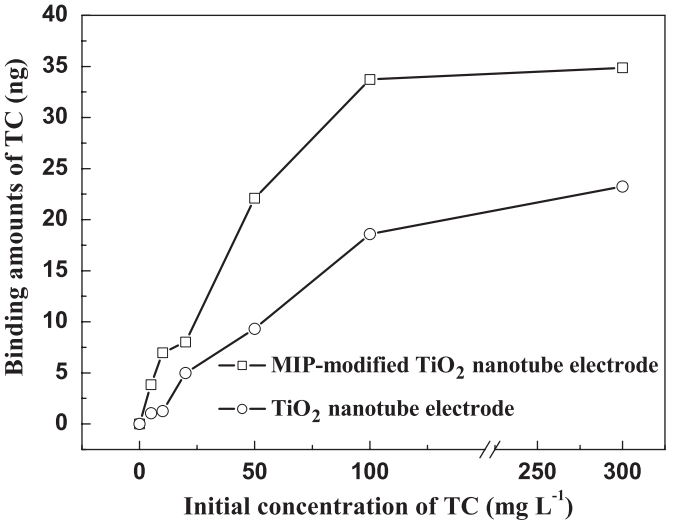


**Fig. 6.** Amount of TC molecules bound by MIP-modified $TiO_2$ nanotube array electrode and $TiO_2$ nanotube array electrode.

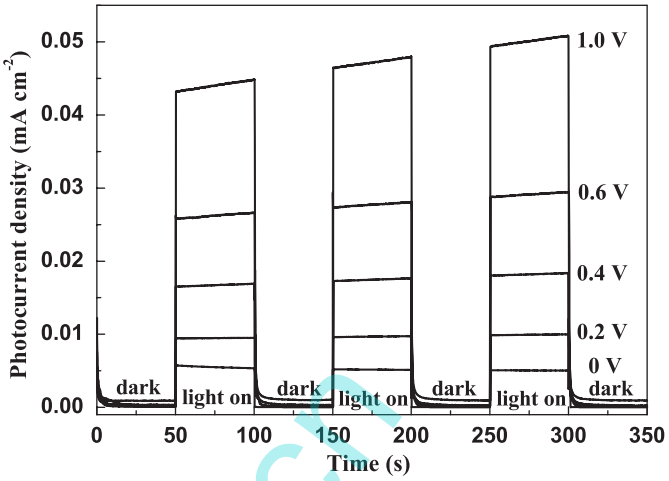


**Fig. 7.** Photocurrent densities vs. time of MIP-modified $TiO_2$ nanotube array electrode being applied with different bias potentials (vs. SCE) under simulated solar light irradiation ($I_0 = 50\,mW\,cm^{-2}$).

with different TC concentrations. The whole process went on with continuous magnetic stirring for 2 h at room temperature. The amount of adsorbed TC was determined by measuring the difference between total TC amount and residual amount in solution. The adsorption capability of $TiO_2$ nanotube arrays for TC was also performed under the same conditions. The imprinting effect could be confirmed by the fact that the MIP-modified $TiO_2$ nanotube arrays showed a higher adsorption capacity for TC than the $TiO_2$ nanotube arrays (Fig. 6), indicating the molecular recognition ability and adsorption ability of MIP [26]. The maximum of adsorption capacity at equilibrium condition was about 34.88 ng for the MIP-modified sample, which was nearly 1.5-fold of that for the $TiO_2$ nanotube arrays. The effective imprinted sites produced at the wall or in the inside surface of the nanotubes contributed to the improved adsorption capacity of MIP-modified $TiO_2$ nanotube arrays to target molecules.

### 3.6. *Photoelectrochemical characteristics of MIP-modified $TiO_2$ nanotube arrays*

According to DRS analysis, the absorption edge of MIP-modified electrode extended to the visible light region. Therefore, the photoelectrochemical measurements of MIP-modified $TiO_2$ nanotube array electrode were carried out using 0.5 M sodium sulfate as the supporting electrolyte to measure the photoresponse of the electrode under simulated solar light irradiation. The difference between the dark and the light currents is the photocurrent [32]. As indicated in Fig. 7, no current was observed on the MIP-modified $TiO_2$ nanotube array electrode in the dark. While under simulated solar light irradiation and no bias potential being applied on MIP-modified photoanode, an average $0.507 \times 10^{-2}\,mA\,cm^{-2}$ photocurrent density on the photoanode was observed. When 0.2, 0.4, 0.6 and 1.0 V (vs. SCE) were applied to the MIP-modified photoanode, the photocurrent densities were increased to average $0.986 \times 10^{-2}$, $1.80 \times 10^{-2}$, $2.87 \times 10^{-2}$ and $4.93 \times 10^{-2}\,mA\,cm^{-2}$, respectively. The generation of the photocurrent should be ascribed to the MIP-modified $TiO_2$ nanotube array electrode response to the solar light.

The photocurrent densities on MIP-modified $TiO_2$ nanotube array electrode in the supporting electrolytes with and without TC were also measured under simulated solar light irradiation as shown in Fig. 8. It was clear that the photocurrent density in the

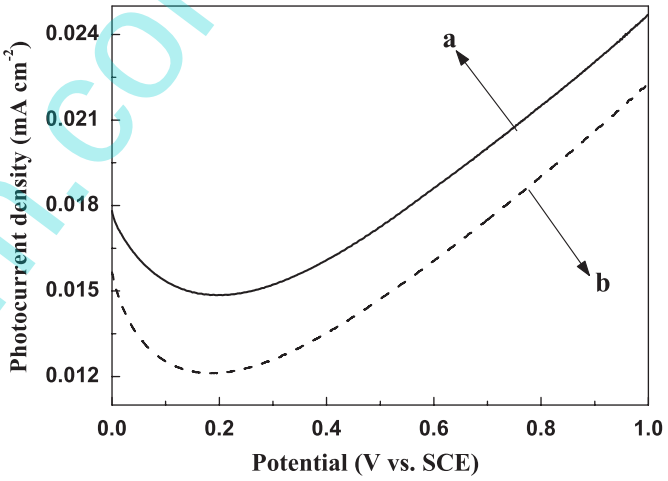


**Fig. 8.** Photocurrent density generation of MIP-modified $TiO_2$ nanotube array electrode in: (a) water solution containing 5 mg $L^{-1}$ TC and (b) pure water solution under simulated solar light irradiation ($I_0 = 50\,mW\,cm^{-2}$).

electrolyte containing TC was higher than that in pure water, which meant that the presence of TC promoted the separation of photogenerated electrons and holes. The reason might be as follows: photogenerated holes can react with water to produce ·OH, which can oxidize the TC effectively. The decrease of the amount of ·OH will promote the reaction Eq. (1):

$$h^+ + H_2O \rightarrow \cdot OH + H^+ \quad (1)$$

Then more photogenerated holes are formed and further involved in the reaction Eq. (1) to create ·OH. Therefore, the combination of photogenerated carriers is inhibited to some extent and more photogenerated electrons are driven to the counter electrode, leading to a significant increase in the photocurrent. In this process, the adsorption of TC on the MIP-modified electrode contributes to the generation of the higher photocurrent.

### 3.7. *Photoelectrocatalytic activities*

The PC and PEC activities of MIP-modified $TiO_2$ nanotube array electrode were measured under simulated solar light irradiation to

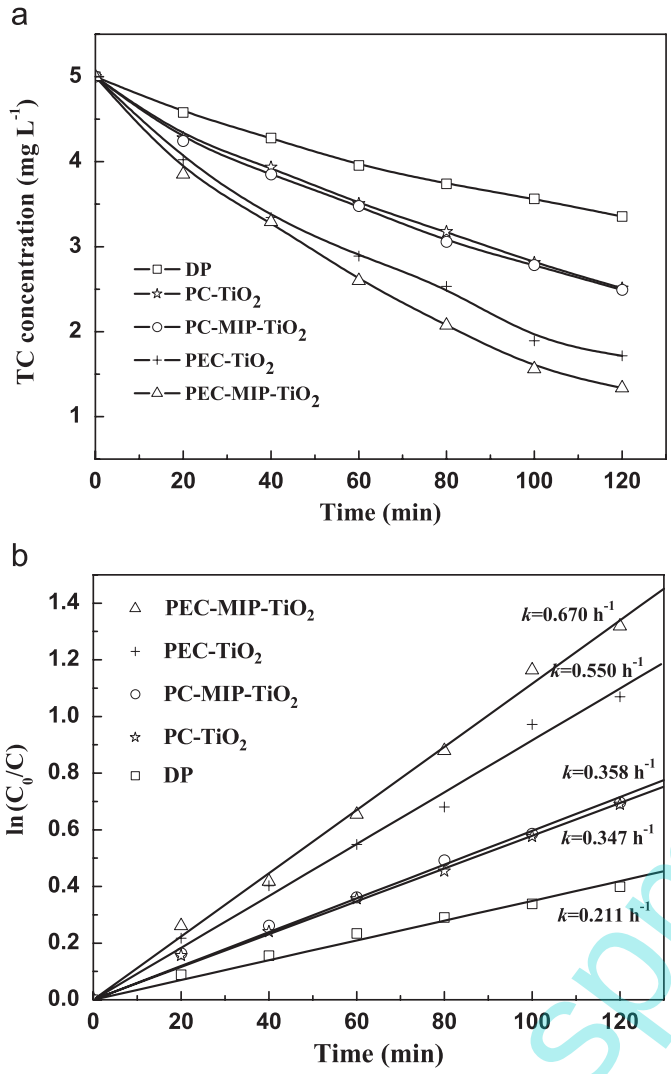


**Fig. 9.** (a) The variation of TC concentrations and (b) the variation of $\ln(C_0/C)$ with degradation time in DP, PC and PEC processes involving MIP-modified $TiO_2$ nanotube array electrode and $TiO_2$ nanotube array electrode under simulated solar light irradiation.

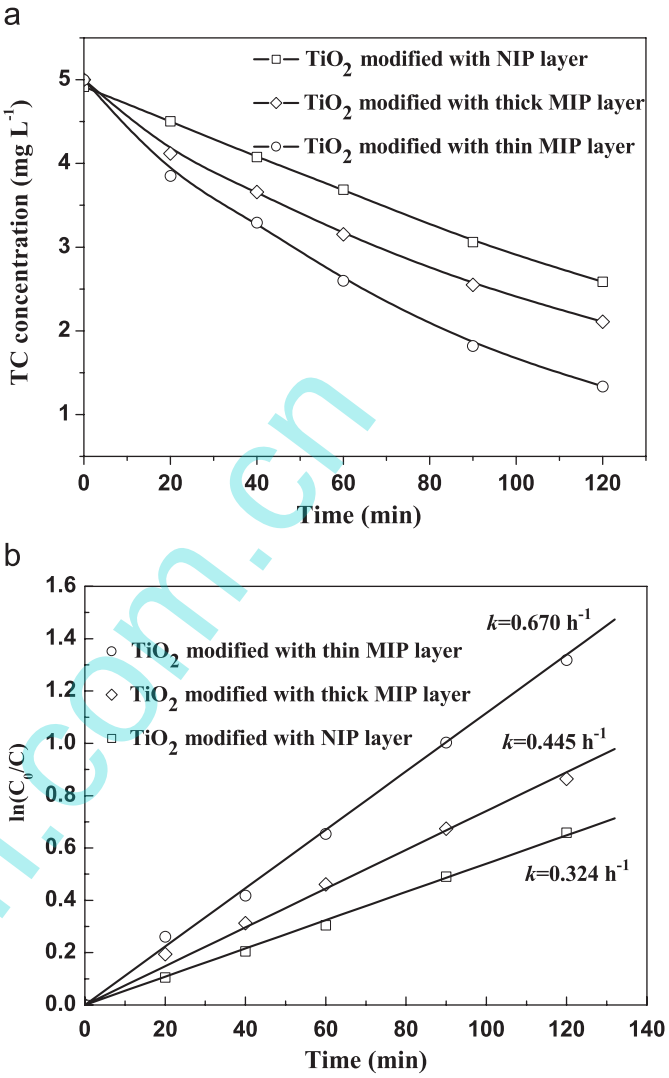


**Fig. 10.** (a) The variation of TC concentrations and (b) the variation of $\ln(C_0/C)$ with degradation time in PEC oxidation under simulated solar light irradiation with NIP-modified $TiO_2$ nanotube array electrode, $TiO_2$ nanotube array electrode modified with thick MIP layer and $TiO_2$ nanotube array electrode modified with thin MIP layer.

investigate their utilization of clean energies such as solar energy. The PC removals of TC on the MIP-modified $TiO_2$ nanotube array electrode and $TiO_2$ nanotube array electrode were almost the same (Fig. 9(a)). Although the adsorption capability of MIP-modified sample is higher than $TiO_2$, the light intensity of the surface of $TiO_2$ nanotube arrays will be weakened due to the absorption of solar light by MIP layer. Their corporate effect may cause similar PC activities of the two electrodes. While in PEC oxidation with a bias potential (0.4 V vs. SCE) being applied, the MIP-modified electrode exhibited better PEC activity than $TiO_2$ electrode. After 2 h, 73% of TC was removed, which was 12% higher than that on $TiO_2$ electrode. It can be explained that the photogenerated carriers are separated efficiently in PEC process, which accelerates the removal of adsorbed TC on the MIP-modified electrode, and more target compounds in the solution are continuously adsorbed on the electrode. The good adsorption capacity of MIP layer modified on the $TiO_2$ nanotube arrays contributes to the relatively higher TC removal. On the other hand, the TOC removal (46%) on MIP-modified electrode after 2 h was lower than TC removal (73%), but it was still 1.5-fold of TOC removal (31%) on $TiO_2$ electrode. Therefore, not only the TC removal efficiency but also the mineralization of TC on the MIP-modified $TiO_2$ nanotube array electrode was increased in the PEC process.

The kinetics of TC degradation in the present study in direct photolysis (DP), PC and PEC processes followed pseudo-first-order kinetics and is described in Fig. 9(b). The apparent first-order rate constant $k$ was evaluated according to $\ln(C_0/C) = kt$, where $C$ represented the TC concentration at time $t$ and $C_0$ was the initial concentration. As shown in Fig. 9(b), the TC could be transformed in DP process, corresponding to the apparent first-order rate constant ($k$) of 0.211 $h^{-1}$. The presence of MIP-modified and neat $TiO_2$ nanotube array electrode increased the rates of TC removals, yielding apparent constants of 0.358 and 0.347 $h^{-1}$, respectively. While in PEC process, the rate of TC removal was further increased. The corresponding apparent first-order rate constant on MIP-modified $TiO_2$ nanotube array electrode was 0.670 $h^{-1}$, approximately 1.2-fold of that on $TiO_2$ nanotube array electrode (0.550 $h^{-1}$).

The influence of polymer layer on PEC activity of $TiO_2$ nanotube electrode was also investigated. As shown in Fig. 10(a), 47%, 58% and 73% of TC were removed in PEC process on NIP-modified electrode, the electrodes modified with thick and thin MIP layers,

respectively. Clearly, the TC removal on NIP-modified electrode was the lowest among these electrodes due to its poor adsorption of the target compound. On the other hand, the MIP-layer thickness would affect the formation of effective imprinted sites in imprinted polymer shells and sequentially the adsorption capacity of MIP layer [33], which played a role in determining the PEC activity of MIP-modified $TiO_2$ nanotube electrode. The PEC activity of the electrode modified with thick MIP layer was inferior to the one modified with thin MIP layer, indicating that more bulk aggregates formed in the polymer could reduce the amount of effective imprinted sites and thus the accessibility of the target species; and besides, the thick MIP layer would weaken the simulated solar light more deeply, which was also unfavorable to PEC degradation. The reaction kinetics is undergone by linear fit and corresponding kinetic constants are shown in Fig. 10(b). The fastest TC removal rate was obtained on $TiO_2$ nanotube array electrode modified with thin MIP layer, corresponding to the apparent first-order rate constant ($k$) of 0.670 $h^{-1}$, roughly 1.5- and 2-fold of those on the electrode modified with thick MIP layer (0.445 $h^{-1}$) and NIP-modified $TiO_2$ nanotube array electrode (0.324 $h^{-1}$), respectively.

## 4. Conclusions

In the present study, an MIP-modified $TiO_2$ nanotube array electrode was prepared. The MIP layer provided the $TiO_2$ electrode molecular adsorption ability, leading to higher adsorption capability for TC. Moreover, MIP modification also enhanced $TiO_2$ nanotube array response to simulated solar light. The experimental results confirmed that the PEC activity of $TiO_2$ electrode under simulated solar light irradiation could be improved by molecular imprinting technique at $TiO_2$ nanotube arrays. This study provides a viable approach for producing surface modified $TiO_2$ nanotube array electrode that is expected to be promising in solar energy related practical applications.

## Acknowledgments

This work was supported jointly by the National Nature Science Foundation of China (No. 20507003), the National Science Fund for Distinguished Young Scholars of China (No. 20525723), and the Hi-Tech research and development program of China (No. 2007AA06Z406).

## References

[1] K. Vinodgopal, S. Hotchandani, P.V. Kamat, J. Phys. Chem. 97 (1993) 9040–9044.
[2] X.Z. Li, H.L. Liu, P.T. Yue, Environ. Sci. Technol. 34 (2000) 4401–4406.
[3] X. Quan, S.G. Yang, X.L. Ruan, H.M. Zhao, Environ. Sci. Technol. 39 (2005) 3770–3775.
[4] R.J. Candal, W.A. Zeltner, M.A. Anderson, J. Adv. Oxid. Technol. 3 (1998) 270–276.
[5] R.J. Candal, W.A. Zeltner, M.A. Anderson, Environ. Sci. Technol. 34 (2000) 3443–3451.
[6] R.M. Torresi, O.R. Camara, C.P. De Pauli, M.C. Giordano, Electrochim. Acta 32 (1987) 1291–1301.
[7] S.P. Albu, A. Ghicov, J.M. Macak, R. Hahn, P. Schmuki, Nano Lett. 7 (2007) 1286–1289.
[8] A.J. Frank, N. Kopidakis, J. van de Lagemaat, Coordin. Chem. Rev. 248 (2004) 1165–1179.
[9] G.K. Mor, K. Shankar, M. Paulose, O.K. Varghese, C.A. Grimes, Nano Lett. 6 (2006) 215–218.
[10] H.F. Zhuang, C.J. Lin, Y.K. Lai, L. Sun, J. Li, Environ. Sci. Technol. 41 (2007) 4735–4740.
[11] Y. Yu, J.C. Yu, C.Y. Chan, Y.K. Che, J.C. Zhao, L. Ding, W.K. Ge, P.K. Wong, Appl. Catal. B: Environ. 61 (2005) 1–11.
[12] C.G. Xie, Z.P. Zhang, D.P. Wang, G.J. Guan, D.M. Gao, J.H. Liu, Anal. Chem. 78 (2006) 8339–8346.
[13] G. Vlatakis, L.I. Andersson, R. Müller, K. Mosbach, Nature 361 (1993) 645–647.
[14] B. Sellergren, Angew. Chem. Int. Ed. 39 (2000) 1031–1037.
[15] C.J. Percival, S. Stanley, M. Galle, A. Braithwaite, M.I. Newton, Anal. Chem. 73 (2001) 4225–4228.
[16] K. Haupt, K. Mosbach, Chem. Rev. 100 (2000) 2495–2504.
[17] L. Feng, Y.J. Liu, J.M. Hu, Langmuir 20 (2004) 1786–1790.
[18] N.M. Bergmann, N.A. Peppas, Prog. Polym. Sci. 33 (2008) 271–288.
[19] C.Y. Li, C.F. Wang, C.H. Wang, S.S. Hu, Sens. Actuators B: Chem. 117 (2006) 166–171.
[20] C.G. Xie, B.H. Liu, Z.Y. Wang, D.M. Gao, G.J. Guan, Z.P. Zhang, Anal. Chem. 80 (2008) 437–443.
[21] G.J. Guan, Z.P. Zhang, Z.Y. Wang, B.H. Liu, D.M. Gao, C.G. Xie, Adv. Mater. 19 (2008) 2370–2374.
[22] S.C. Zimmerman, M.S. Wendland, N.A. Rakow, I. Zharov, K.S. Suslick, Nature 418 (2002) 399–403.
[23] G. Wulff, Chem. Rev. 102 (2002) 1–28.
[24] A. Katz, M.E. Davis, Nature 403 (2000) 286–289.
[25] E. Mertz, S.C. Zimmerman, J. Am. Chem. Soc. 125 (2003) 3424–3425.
[26] X.T. Shen, L.H. Zhu, J. Li, H.Q. Tang, Chem. Commun. (2007) 1163–1165.
[27] X.T. Shen, L.H. Zhu, G.X. Liu, H.W. Yu, H.Q. Tang, Environ. Sci. Technol. 42 (2008) 1687–1692.
[28] G.K. Mor, O.K. Varghese, M. Paulose, K. Shankar, C.A. Grimes, Sol. Energy Mater. Sol. C 90 (2006) 2011–2075.
[29] K. Kummerer, A.A. Ahmad, V.M. Sundermann, Chemosphere 40 (2000) 701–710.
[30] C. Tixier, H.P. Singer, S. Oellers, S.R. Muller, Environ. Sci. Technol. 37 (2003) 1061–1068.
[31] N. Lu, X. Quan, J. Li, S. Chen, H. Yu, G. Chen, J. Phys. Chem. C 111 (2007) 11836–11842.
[32] J.A. Byrne, B.R. Eggins, J. Electroanal. Chem. 457 (1998) 61–72.
[33] D.M. Gao, Z.P. Zhang, M.H. Wu, C.G. Xie, G.J. Guan, D.P. Wang, J. Am. Chem. Soc. 129 (2007) 7859–7866.